

SUPPLEMENTAL MATERIALS

MYSM1 Maintains Ribosomal Protein Gene Expression in Hematopoietic Stem Cells to Prevent Hematopoietic Dysfunction

*Jad I Belle ^{1,2}, *HanChen Wang ^{1,2,3}, Amanda Fiore ^{1,2}, Jessica C Petrov ^{1,2}, Yun Hsiao Lin ^{1,2}, Chu-Han Feng ^{1,2}, Thi Tuyet Mai Nguyen ⁴, Jacky Tung ^{1,2}, Philippe M Campeau ⁴, Uta Behrends ⁵, Theresa Brunet ⁶, Gloria Sarah Leszinski ^{6,7}, Philippe Gros ^{2,8,9}, #David Langlais ^{2,3,10}, #Anastasia Nijnik ^{1,2}

¹ Department of Physiology, McGill University, Montreal, QC, Canada

² McGill University Research Centre on Complex Traits, McGill University, QC, Canada

³ Department of Human Genetics, McGill University, Canada

⁴ Centre Hospitalier Universitaire St. Justine Research Center, University of Montreal, QC, Canada

⁵ Childrens' Hospital, Technische Universität München, Munich, Germany

⁶ Institute of Human Genetics, Technische Universität München, Munich, Germany

⁷ Institute of Human Genetics, Helmholtz Zentrum München, Neuherberg, Germany

⁸ Department of Biochemistry, McGill University, Canada

⁹ The Rosalind and Morris Goodman Cancer Research Centre, McGill University, Canada

¹⁰ McGill University Genome Centre, Montreal, QC, Canada

* These authors contributed equally to this work

Corresponding authors:

Anastasia Nijnik, 368 Bellini Life Sciences Complex, 3649 Promenade Sir William Osler, McGill University, H3G 0B1 Montreal, QC, Canada. Tel: 1-514-398-5567, Fax: 1-514-398-2603, Email: anastasia.nijnik@mcgill.ca.

David Langlais, Rm 4203, 740 Ave Dr Penfield, McGill University Genome Centre, Montreal, QC, Canada, H3A 0G1. Tel: 1-514-398-5844, Email: david.langlais@mcgill.ca.

TABLE OF CONTENTS

Item	Page
Supplemental Figure Legends 1-10	3-5
Supplemental Tables	6-13
Part I. Supplemental Table Legends 1-6	6-7
Part II. Supplemental Data Tables 7-8	8-9
Part III. Materials and Methods Tables 9-13	10-13
Supplemental Materials and Methods: Flow Cytometry Analyses	14-15
Supplemental Figures 1-10	16-25
Supplemental Tables 1-6 – attached as separate documents	-

SUPPLEMENTAL FIGURE LEGENDS

Figure S1. Flow cytometry gating strategy, used to sort hematopoietic stem cells and multipotent progenitor cells (HSC, MPP1, and MPP2) for RNA-Seq analysis.

(A) Representative flow cytometry density plots, showing the gating on single, live, lineage marker negative cells (Lin^-). (B) Gating on $\text{Lin}^- \text{cKit}^+ \text{Sca1}^+$ (LSK) hematopoietic stem and progenitor cells, followed by the subdivision of this cell population based on CD150 and CD48 marker expression. (C) Analysis of the pre-gated LSK sub-sets for CD34 and Flt3 marker expression, to identify highly pure HSC and MPP1-MPP4 cells. Representative percentages of cells within each gate, relative to the parent gate, are shown.

Figure S2. Expression of *Mysm1*, *RP*-genes, and p53-target genes in the RNA-Seq datasets from *Mysm1*-deficient and control hematopoietic stem cells and multipotent progenitor cells.

(A) Expression of *Mysm1* is reduced along the development of wild type HSC to MPP2 cells. (B) Gene Set Enrichment Analysis (GSEA) demonstrating reduced expression of 80 ribosomal protein genes (*RP*-genes) in wild-type MPP1 and MPP2 cells compared to wild-type HSCs. 10,769 genes expressed in the RNA-Seq dataset are ranked based on signal-to-noise ratio for the HSC, MPP1, and MPP2 cell populations, and each relevant *RP*-gene is represented by a dot and a vertical bar below. (C) Boxplots of the relative Log_2 expression of *RP*-genes also show downregulation in wild type MPP1 and MPP2 cells relative to wild type HSCs. (D) GSEA demonstrating upregulation of p53-target genes in *Mysm1*-deficient HSC, MPP1 and MPP2 cells relative to the corresponding control cells, with increasing upregulation along the HSC to MPP1 to MPP2 differentiation axis.

Figure S3. MYSM1-bound *RP*-gene promoters harbor high levels of H3K27ac and low levels of H2AK119ub. As high gene expression is known to correlate with high levels of H3K27 acetylation and low levels H2AK119 ubiquitination, the data demonstrates that MYSM1-bound *RP*-gene promoters have the epigenetic status of highly active genes. (A) Heat map showing the intensities of H3K27ac and H2AK119ub around all 35,682 mm9 gene transcriptional start sites (TSS) and 2,099 MYSM1 binding sites. The sites around mm9 gene TSS are ranked based on the level of H3K27ac in HPC7 cells. The sites around MYSM1 binding sites are ranked based on their distance to the nearest gene TSS. (B) Box plot displays the read densities of H3K27ac and H2AK119ub peaks around each ribosomal protein gene (*RP*-gene) in HPC7 and Ba/F3 cells.

Figure S4. Epigenetic and transcriptional profiles of additional *RP*-genes, not shown in the main Figure 4. The genes are grouped based on their association with DBA syndrome and MYSM1 regulation, as indicated by MYSM1 binding in proximity to their TSS and dysregulation in expression in *Mysm1*-deficient HSC and MPP cells: (A) MYSM1-regulated DBA-associated *RP*-genes; (B) DBA-associated *RP*-genes with proximal MYSM1-binding sites but non-significant dysregulation in *Mysm1*-deficient HSC and MPP cells; (C) MYSM1-regulated *RP*-genes with no

known association to DBA syndrome; and **(D)** DBA-associated *RP*-genes with no proximal MYSM1 binding sites. Gene structure and names are indicated in the middle section of each panel and DBA-associated genes are highlighted in red; ChIP-Seq tracks are shown above and RNA-Seq tracks below. Averaged gene expression changes in *Mysm1*-deficient relative to wild type cells are indicated by arrows, and the gene expression level normalized per million reads is indicated at the top-right corner.

Figure S5. Flow cytometry gating strategy used to identify hematopoietic stem cells for intracellular protein synthesis rate analyses. **(A)** Representative flow cytometry density plots, showing the gating on single, live, lineage marker negative cells (Lin^-). **(B)** Gating on $\text{Lin}^- \text{cKit}^+ \text{Sca1}^+$ (LSK) hematopoietic stem and progenitor cells, followed by the isolation of the $\text{CD150}^+ \text{Flt3}^- \text{CD34}^-$ stem cell population. Representative percentages of cells within each gate, relative to the parent gate, are shown.

Figure S6. PUMA-independent induction of p53-stress response genes and downregulation of *RP*-genes in *Mysm1*-deficient stem and progenitor cells. **(A)** Partial Least Squares Regression graph of the transcriptome profiles of CD150^+ and CD150^- LSK hematopoietic stem and progenitor cells, isolated from *Mysm1*-deficient *Mysm1*^{-/-}*Puma*^{+/-} and *Mysm1*^{-/-}*Puma*^{-/-}, and control wild type and *Puma*^{-/-} mice. The samples are segregated by cell type on the principal component 1 (PC1) and by *Mysm1* genotype on PC2. **(B)** Heat map displaying 770 genes significantly dysregulated in *Mysm1*-deficient relative to wild type control cells for each cell-type. The threshold for significance is: fold change $\geq |1.5|$ and False Discovery Rate (FDR) ≤ 0.01 . Relative expression to the average of wild type CD150^+ LSK group is used to generate the heat map. Hierarchical Clustering using Pearson correlation and complete linkage is performed to generate the gene clusters (Clusters 1-8). Significantly enriched gene ontology (GO) terms for select gene clusters are shown. Detailed gene lists and GO enrichment analyses can be found in Table S4. **(C)** Gene Set Enrichment Analysis (GSEA) demonstrating reduced expression of 80 *RP*-genes in *Mysm1*^{-/-}*Puma*^{+/-} and *Mysm1*^{-/-}*Puma*^{-/-} hematopoietic progenitor cells (CD150^- LSK) relative to wild type control cells; 10,987 genes expressed in the RNA-Seq dataset are ranked based on signal-to-noise ratio and each relevant *RP*-gene represented by a dot and a vertical bar below. Boxplots of relative Log_2 expression of the *RP*-genes also show downregulation in *Mysm1*^{-/-}*Puma*^{+/-} and *Mysm1*^{-/-}*Puma*^{-/-} cells relative to control cells.

Figure S7. Loss of p21 does not rescue the anemia phenotypes in *Mysm1*-deficiency. The data presented is from wild type, *p21*^{-/-}, *Mysm1*^{-/-}, and *Mysm1*^{-/-}*p21*^{-/-} mice. **(A)** Hematology analysis of erythrocyte counts in peripheral blood of the mice. **(B)** MEP cell numbers in the mouse bone marrow, presented per 1 tibia and femur; cells gated as $\text{Lin}^- \text{cKit}^+ \text{Sca1}^- \text{CD34}^- \text{CD16/32}^- \text{CD127}^-$. **(C)** Hematocrit and blood hemoglobin concentration. **(D)** MCV, MCH, and MCHC parameters. **(E)** Hematology analysis of leukocyte and lymphocyte counts. Mean \pm SEM is presented; statistical

comparisons using ANOVA with Bonferroni post-hoc test; NS - non-significant, * $p < 0.05$, ** $p < 0.01$, *** $p < 0.001$, **** $p < 0.0001$.

Figure S8. Loss of *Bbc3*/PUMA partially rescues anemia phenotype in *Mysm1*-deficiency. The data presented is from wild type, *Puma*^{-/-}, *Mysm1*^{-/-}, and *Mysm1*^{-/-}*Puma*^{-/-} mice, including (A) hematology analysis of erythrocyte counts in mouse blood; (B) MEP cell numbers in the bone marrow, per 1 tibia and femur, gated as Lin⁻cKit⁺Sca1⁻CD34⁻CD16/32⁻CD127⁻; (C) hematocrit and blood hemoglobin concentration; (D) MCV, MCH, and MCHC parameters; (E) hematology analysis of leukocyte and lymphocyte counts in mouse blood. Mean ± SEM is presented from ≥4 mice per genotype; statistical comparisons using ANOVA with Bonferroni post-hoc test; NS - non-significant, * $p < 0.05$, ** $p < 0.01$, *** $p < 0.001$, **** $p < 0.0001$.

Figure S9. Flow cytometry gating strategy for lymphoid cell populations in erythrocyte-depleted human blood. The figure shows representative plots from a healthy control sample, and indicates the average percentage of cells within each gate relative to the parent gate for all healthy controls samples. Gating is hierarchical within in each panel, with each plot gated on a cell population from preceding plot from left to right. (A) Representative flow cytometry density plots, showing the gating on single and live cells, negative for myeloid lineage markers CD14 and CD16. (B) Gating on CD56⁺CD3⁻ NK cells and CD3⁺CD56⁻ T cells (left panel), followed by gating on CD4⁺ and CD8⁺ T cells (right panel). (C) Analyzing the activation status of CD4 and CD8 T cells by CD45RA and CD27 marker expression. (D) Gating on CD19⁺CD20⁺ B cells. (E) Gating on Lin⁻CD34⁺CD38⁻ and Lin⁻CD34⁻CD38⁺ stem and progenitor cells.

Figure S10. Flow cytometry gating strategy for myeloid cell populations in erythrocyte-depleted human blood. The figure shows representative plots from a healthy control sample, and indicates the average percentage of cells within each gate relative to the parent gate for all healthy controls samples. Gating is hierarchical within in each panel, with each plot gated on a cell population from preceding plot from left to right. (A) Plots showing gating on single and live cells, negative for lymphoid lineage markers CD3, CD20 and CD56. (B) Plots showing gating on the following cell populations, from left to right within the panel: CD16⁺CD66b⁺ neutrophils; CD123⁺MHCII⁺ plasmacytoid dendritic cells and CD123⁺MHCII⁻ basophils; CD14^{hi}CD16^{lo} classical monocytes and CD14^{lo}CD16^{hi} non-classical monocytes; and CD11c⁺MHCII⁺ myeloid dendritic cells.

PART I. SUPPLEMENTAL TABLES
TABLE LEGENDS 1-6 (with tables attached as separate files)

Table S1. Differentially expressed gene list and gene ontology enrichment analyses for the *Mysm1^{fl/fl}* CreERT2 RNA-Seq dataset; related to Figures 1E-F. (A) List of genes differentially expressed in HSC, MPP1 and MPP2 cells from tamoxifen treated *Mysm1^{fl/fl}* CreERT2 relative to control mice; related to Figure 1E. Information provided for each gene includes: the cluster information, heatmap row number (Figure 1E), gene name, fold change, log2 fold change, false discovery rate (FDR), and normalized counts per million. (B) Full list of genes expressed in HSC, MPP1 and MPP2 cells from tamoxifen treated *Mysm1^{fl/fl}* CreERT2 and control mice; same information as in (A) is provided for each gene. (C-N) Gene ontology enrichment analyses showing the enriched biological process (BP), cellular component (CC), and molecular function (MF) terms for each cluster of differentially expressed genes from Figures 1E-F.

Table S2. Gene set enrichment analysis results for the *Mysm1^{fl/fl}* CreERT2 RNA-Seq dataset; related to Figure 1D. Normalized enrichment scores (NES) of 4,436 pre-established biological processes signatures used in the gene set enrichment analysis and depicted in Figure 1D. In each column, positive values indicate biological process terms upregulated in *Mysm1^{Δ/Δ}* relative to control cells, and negative values indicate terms downregulated in *Mysm1^{Δ/Δ}* relative to control cells.

Table S3. Consolidation of MYSM1 ChIP-Seq and *Mysm1^{fl/fl}* CreERT2 RNA-Seq datasets; related to Figure 4A. Putative MYSM1-regulated genes are identified as having MYSM1-binding peaks in ChIP-Seq data, and significant dysregulation in expression in *Mysm1^{Δ/Δ}* relative to control cells in the RNA-Seq data. Information provided includes: MYSM1 peak set, dysregulated gene cluster, and search window. Locations of gene TSSs within the search window for each MYSM1 peak are shown. Note that a peak can have more than one gene TSS within the search window.

Table S4. Differentially expressed gene list and gene ontology enrichment analyses for the *Mysm1^{-/-}Puma^{-/-}* RNA-Seq dataset; related to Figure S6. (A) List of genes differentially expressed in the RNA-Seq dataset comparing samples of *Mysm1^{-/-}Puma^{+/-}*, *Mysm1^{-/-}Puma^{-/-}*, *Puma^{-/-}* and control wild-type genotypes for each cell type; the significance threshold is $FC \geq \pm 1.5$ and $FDR \leq 0.01$. Information provided for each gene includes: the clustering information, row number on the heatmap in Figure S6B, gene name, fold change, log2 fold change, false discovery rate (FDR), and normalized counts per million. (B) Full list of genes expressed in the RNA-Seq dataset; same information as in (A) is provided for each gene. (C-J) Gene ontology enrichment analyses showing the enriched biological process (BP) terms for each cluster of differentially expressed genes 1-8 shown in Figure S6B.

Table S5. Hematological and genetic characterization of the index patient; related to Figure 8. (A) Longitudinal hematological profile of the index (II-4) patient performed during clinical monitoring. Episode of transfusions are indicated in the table. (B) Exome sequencing report for

the index (II-4) patient. Exome sequence data were analyzed and filtered as described in the Methods. Variant prioritization was performed based on an autosomal recessive pattern of inheritance (homozygous or compound heterozygous with a minor allele frequency <0.1%; and excluding variants with multiple homozygous occurrences in gnomAD). We have also searched for autosomal dominant pattern of inheritance (heterozygous with a minor allele frequency <0.001% which could not be identified in the parents).

Table S6. Comparison of the clinical features of the index patient and the diagnostic criteria of major human ribosomopathy syndromes; Related to Figure 8.

PART II. SUPPLEMENTAL TABLES
DATA TABLES 7-8

Table S7. Frequencies of major cell types in the blood of MYSM1-deficient index patient and healthy controls; related to Figure 8D. The control figure represents mean (\pm S.D.) of three independent biological samples and the patient figure represents the average of three technical replicates from a single blood sample. Cell populations depleted in the index patient relative to control are highlighted in green, and those increased in relative frequency highlighted in orange.

Cell Population	Statistic	Control	p.Ser290* (hom)
Live	% of cells	86% (\pm 1)	72%
Neutrophils	% of live	42% (\pm 17)	4%
Basophils	% of live	0.4% (\pm 0.05)	0.03%
Monocytes (classical)	% of live	1.3% (\pm 0.2)	0.3%
Monocytes (non-classical)	% of live	2.9% (\pm 1.5)	3.0%
Myeloid dendritic cells	% of live	0.24% (\pm 0.05)	0.20%
Plasmacytoid dendritic cells	% of live	0.09% (\pm 0.02)	0.15%
B cells	% of live	2.2% (\pm 0.5)	0.9%
- memory	% of B cells	17% (\pm 7)	7%
CD4 T cells	% of live	23% (\pm 5)	57%
- naïve	% CD4 T cells	69% (\pm 7)	91%
- effector	% CD4 T cells	8% (\pm 3)	1.2%
- memory	% CD4 T cells	21% (\pm 5)	5%
CD8 T cells	% of live	12% (\pm 5)	21%
- naïve	% CD8 T cells	61% (\pm 20)	94%
- effector	% CD8 T cells	14% (\pm 8)	0.7%
- memory	% CD8 T cells	10% (\pm 4)	3%
NK cells	% of live	1.8% (\pm 0.7)	1.0%
Lin ⁻ CD34 ⁺ CD38 ⁻ stem cells	% of live	0.19% (\pm 0.13)	0.22%
Lin ⁻ CD34 ⁺ CD38 ⁺ progenitor cells	% of live	0.43% (\pm 0.02)	0.49%

Table S8. Measurements of cellular protein synthesis rates and the levels of p53 protein in the leukocytes of MYSM1-deficient index patient and healthy controls; related to Figure 8E-F. Protein synthesis rate is measured using the O-propargyl-puromycin (OPP) incorporation method; mean fluorescence intensity (MFI) of the cells is presented, with the control figure representing mean (\pm S.D.) of three independent biological samples and the patient figure representing a single measurement. Reduction in the patient samples relative to controls is indicated in green, and increase in orange.

Cell Type	MFI - Protein Synthesis		MFI - p53	
	WT	p.Ser290*	WT	p.Ser290*
B cells	10,419 (\pm 2,483)	2,864	556 (\pm 275)	1,121
CD4 T cells	14,304 (\pm 2,096)	6,549	470 (\pm 197)	636
CD8 T cells	13,031 (\pm 1,632)	4,801	608 (\pm 289)	788
NK cells	7,649 (\pm 1,973)	2,795	861 (\pm 304)	1,305
Neutrophils	15,999 (\pm 5,339)	21,426	5,465 (\pm 974)	7,529
Basophils	12,328 (\pm 1,524)	1,417	893 (\pm 248)	3,058
Monocytes - classical	18,089 (\pm 5,737)	4,079	1,431 (\pm 713)	1,086
Monocytes - non-classical	6,840 (\pm 3,026)	3,791	1,113 (\pm 279)	2,072
Dendritic cells - myeloid	11,926 (\pm 3,048)	11,588	1,138 (\pm 893)	1,020
Dendritic cells - plasmacytoid	32,059 (\pm 5,536)	22,392	1,844 (\pm 801)	1,835
Progenitors	11,501 (\pm 1,391)	7,878	699 (\pm 306)	2,323
Stem cells	9,462 (\pm 2,813)	3,597	930 (\pm 603)	1,268

**PART III. SUPPLEMENTAL TABLES
METHODS TABLES 9-13**

Table S9. RT-qPCR Primers Sequences.

Target Gene	Forward Sequence	Reverse Sequence
<i>Rps3</i>	ctgaaggcagcgtagagctt	tccaaggagttttagcgtaga
<i>Rps10</i>	gtgagcgacctgcaagattc	cagcctcagctttctgtca
<i>Rps24</i>	gcagtgagcggctcctttt	gggccggatggttactgtgt
<i>Rpl7</i>	ccttgattgctcggctctt	agcctgtttatctggcttcc
<i>Rpl9</i>	catccaggagaatggctcttt	cagttccctctcagacacatag
<i>Rpl11</i>	aatgagaagattgctgttactg	caactcatactcccgcacct
<i>Rpl13</i>	gaaacaagtccacggagtc	ttgctcggatgccaaaga
<i>Eef1g</i>	tcacgagaggagaacagaaac	cagggaccagccatctttatc
<i>Hprt</i>	caggccagactttgttgat	ttgcgctcatcttaggcttt
<i>Mysm1</i>	gggattccgacctactgtc	tggaaaggaacagattttctattg

Table S10. ChIP Antibodies.

Antigen	ID	Supplier	Origin
FLAG	F1804	Sigma-Aldrich®	Mouse monoclonal
H2AK119ub	D27C4	Cell Signaling Technology®	Rabbit monoclonal
H3K27ac	ab4729	Abcam®	Rabbit polyclonal
H3	ab1791	Abcam®	Rabbit polyclonal

Table S11. ChIP-qPCR Primer Sequences.

Target Region	Forward Sequence	Reverse Sequence
<i>Rps3</i> 98 bp downstream (Chr7:106,631,961-106,632,121)	aatacacaatctacggccatcc	agattccaagaagaggaaggaag
<i>Rps10</i> 199 bp downstream (Chr17:27,771,920-27,771,988)	gtggccttcaaactcctctc	actcagagtcgactgaagaaga
<i>Rps24</i> 0 bp upstream TSS (5'UTR) (Chr14:25,309,903-25,310,020)	cttgcgcggtgatgatgattgg	gataagcgacggatagtgctg
<i>Rpl7</i> 141 bp downstream (Chr1:16,094,250-16,094,373)	ctcagttgctcctggactg	tgtatctgagtgtagcctgga
<i>Rpl9</i> 8 bp upstream (Chr5:65,782,562-65,782,678)	caaacagaggatgggtcagatt	gccctgacggattacaagaac
<i>Rpl11</i> 70 bp upstream (Chr4:135,609,214-135,609,356)	cggatggagacggatgaaag	ctcgttgtctgcctagaagaa
<i>Rpl13</i> 18 bp upstream (Chr8:125,626,232-125,626,358)	cacttcccttcgcctgattt	ggcagagactcacctctatac
<i>Eef1g</i> 197 bp downstream (Chr19:9,041,728-9,041,874)	gctccggtgattaggggtcac	ctccaggccctagaaccat
<i>POMC</i> 744 bp downstream (Chr12:3,953,603-3,955,695)	aggcagatggacgcacataggtaa	tccacttagaactggacagaggct

Table S12. Antibodies for Flow Cytometry Analyses of Human Blood.

Target	Fluorophore	Clone	Supplier
CD3	PE	UCHT1	BioLegend
CD3	Brilliant Violet 605	SK7	BioLegend
CD4	PE-Dazzle 594	RPA-T4	BioLegend
CD8	APC-Cy7	HIT8a	BioLegend
CD11c	Brilliant Violet 421	Bu15	BioLegend
CD14	PE-Dazzle 594	HCD14	BioLegend
CD14	Alexa Fluor 700	HCD14	BioLegend
CD16	Brilliant UV 737	3G8	BD BioSciences
CD16	Alexa Fluor 700	3G8	BioLegend
CD19	PerCP-Cy5.5	HIB19	BioLegend
CD20	PE	2H7	BioLegend
CD27	Brilliant UV 737	L128	BD BioSciences
CD34	PE-Cy7	561	BioLegend
CD38	Brilliant Violet 711	HIT2	BioLegend
CD45RA	Brilliant Violet 421	HI100	BioLegend
CD56	PE	HCD56	BioLegend
CD56	Brilliant UV 395	NCAM 16.2	BD BioSciences
CD66b	PerCP-Cy5.5	G10F5	BioLegend
CD123	Brilliant UV 395	7G3	BD BioSciences
HLA-DR	PE-Cy7	L243	BioLegend
p53	Alexa Fluor 488	1C12	Cell Signaling Technologies

Table S13. Gating Strategies for Flow Cytometry Analyses of Human Blood.

The gating strategy is further presented in Figures S9 and S10.

Cell Populations	Gating Strategy	
	Negative Lineage Gates	Primary Population Gating
Neutrophils	CD20 ⁻ CD3 ⁻ CD56 ⁻	CD66b ⁺ CD16 ⁺
Basophils	CD20 ⁻ CD3 ⁻ CD56 ⁻ & CD66b ⁻	CD123 ⁺ HLA-DR ⁻
Plasmacytoid Dendritic Cells	CD20 ⁻ CD3 ⁻ CD56 ⁻ & CD66b ⁻	CD123 ⁺ HLA-DR ⁺
Myeloid Dendritic Cells	CD20 ⁻ CD3 ⁻ CD56 ⁻ & CD66b ⁻	CD11c ⁺ CD14 ⁻ HLA-DR ⁺
Monocytes	CD20 ⁻ CD3 ⁻ CD56 ⁻ & CD66b ⁻	CD14 ⁺ CD16 ^{+/-} HLA-DR ⁺
CD4 T cells	CD14 ⁻ CD16 ⁻ & CD56 ⁻	CD3 ⁺ CD4 ⁺ CD8 ⁻
Naïve CD4 T cells	CD14 ⁻ CD16 ⁻ & CD56 ⁻	CD3 ⁺ CD4 ⁺ CD8 ⁻ & CD27 ⁺ CD45RA ⁺
CD8 T cells	CD14 ⁻ CD16 ⁻ & CD56 ⁻	CD3 ⁺ CD4 ⁻ CD8 ⁺
Naïve CD8 T cells	CD14 ⁻ CD16 ⁻ & CD56 ⁻	CD3 ⁺ CD4 ⁻ CD8 ⁺ & CD27 ⁺ CD45RA ⁺
NK cells	CD14 ⁻ CD16 ⁻ & CD3 ⁻	CD56 ⁺
B cells	CD14 ⁻ CD16 ⁻ & CD3 ⁻ CD56 ⁻	CD20 ⁺ CD19 ⁺
Naïve B cells	CD14 ⁻ CD16 ⁻ & CD3 ⁻ CD56 ⁻	CD20 ⁺ CD19 ⁺ & CD27 ⁻
Stem Cells	CD20 ⁻ CD3 ⁻ CD56 ⁻ & CD14 ⁻ CD16 ⁻	CD34 ⁺ CD38 ⁻
Progenitor Cells	CD20 ⁻ CD3 ⁻ CD56 ⁻ & CD14 ⁻ CD16 ⁻	CD38 ⁺ CD34 ⁻

SUPPLEMENTAL MATERIALS AND METHODS

Flow Cytometry Characterization of Mouse Cells and Tissues

Cell suspensions of mouse bone marrow were prepared in RPMI-1640 (Wisent) with 2% (v/v) FCS, 100µg/ml streptomycin and 100U/ml penicillin (Wisent). The cells were stained for surface-markers in PBS with 2% FCS and 0.2% (w/v) sodium azide for 20 minutes on ice, with the following antibodies: FITC CD16/32 (clone 93, eBioscience), PE CD127 (A7R34, eBioscience), APC Sca-1 (D7, eBioscience), eFluor450 CD34 (RAM34, eBioscience), PE-Cy7 cKit/CD117 (2B8, BioLegend), and PerCP/Cy5.5 lineage markers B220 (RA3-6B2), CD11b (M1/70), TER119 (TER119), CD4 (RM4-5), and CD8a (53-6.7, all from BioLegend). Fixable Viability Dye eFluor506 (eBioscience) was used to discriminate dead cells, and compensation done with BD™ CompBeads (BD Biosciences).

Intracellular staining was performed as previously described (21, 28). The cells were stained with Fixable Viability Dye eFluor506, APC Sca-1 (D7), eFluor450 cKit/CD117 (2B8), and PE CD150 (mShad150, all from eBioscience). The cells were fixed in 2% paraformaldehyde (PFA) in PBS with 2% FCS at 37°C for 10 minutes, and permeabilized in 90% methanol for 30 minutes on ice. The cells were then stained with PerCP/Cy5.5-conjugated antibodies against lineage markers, and either Alexa Fluor 488 anti-p53 (clone 1C12, Cell Signaling Technology), or unconjugated anti-eEF1G (EPR7200, Abcam) followed by Alexa Fluor 488 anti-rabbit IgG secondary antibody (Life Technologies), or appropriate isotype controls. Alternatively, the cells were pre-stained with Fixable Viability Dye eFluor506 (eBioscience), PerCP/Cy5.5-conjugated antibodies against lineage markers, PE-Cy7 cKit/CD117 (2B8, BioLegend), APC-Cy7 Sca1 (D7, BioLegend), APC CD150 (mShad, eBioscience), eFluor450 CD48 (HM48-1, eBioscience), and PE CD135/FLT3 (A2F10, BioLegend), followed by the fixation and permeabilization with the BD Cytotfix/Cytoperm kit (BD Biosciences) according to the manufacturer's protocol, and the staining for intracellular proteins as described above. All data were acquired on FACS Canto II (BD Biosciences) and analyzed with FACS Diva (BD Biosciences) or FlowJo (Tree Star) software.

Flow Cytometry Characterization of the Human Blood

Human blood was collected from the index patient and three unrelated healthy volunteers into the BD Vacutainer Blood Collection Tube - ACD Solution, B Additive, 6 mL Glass Tube (Becton Dickinson). The blood was depleted of erythrocytes using the EasySep™ RBC Depletion Reagent (Stem Cell Technologies), according to manufacturer's protocol. The remaining leukocytes were stained with Fixable Viability Dye eFluor506 (eBioscience, ThermoFisher Scientific), and then for cell surface markers using the antibodies in Table S12. For intracellular analyses of p53 protein levels the samples were fixed and permeabilized using the Transcription Factor Staining Buffer Set (eBiosciences, ThermoFisher Scientific) according to the manufacturer's protocol and stained with anti-p53 Alexa Fluor 488 antibody (clone 1C12, Cell Signaling Technologies) or mouse IgG1 Alexa Fluor 488 isotype control (clone MOPC-21, BioLegend) for 1 hour at room temperature.

The data was acquired on BD LSR Fortessa (BD Biosciences) and analyzed using FlowJo software (Flow Jo, LLC), using the gating strategies summarized in Table S13.

The analyses of cellular protein synthesis rates was performed using the O-propargyl-puromycin (OPP) incorporation method. The leukocytes were rested in RPMI-1640 (Wisent) with 10% fetal calf serum (Wisent), 2mM L-Glutamine, 100 μ g/mL streptomycin, 100U/mL penicillin (Wisent), and 10⁻⁵M β -mercaptoethanol (Sigma-Aldrich) for 45 minutes at 37°C and 5% CO₂. OPP (Invitrogen, ThermoFisher Scientific) was subsequently added to the culture media at the final concentration of 20 μ M and the cells were incubated for further 30 minutes at 37°C and 5% CO₂. The cells were stained with Fixable Viability Dye eFluor506 (eBioscience, ThermoFisher Scientific) and for cell surface markers using the antibodies in Table S12. The cells were fixed and permeabilized using the BD Cytfix/Cytoperm Fixation and Permeabilization Kit (BD Biosciences) according to manufacturer's protocols, and stained for OPP incorporation using the Click-iT Plus OPP Alexa Fluor 647 Protein Synthesis Assay Kit (Invitrogen, ThermoFisher Scientific). The data was acquired on BD LSR Fortessa (BD Biosciences) and analyzed using FlowJo software (Flow Jo, LLC), using the gating strategies summarized in Table S13.

Figure S1

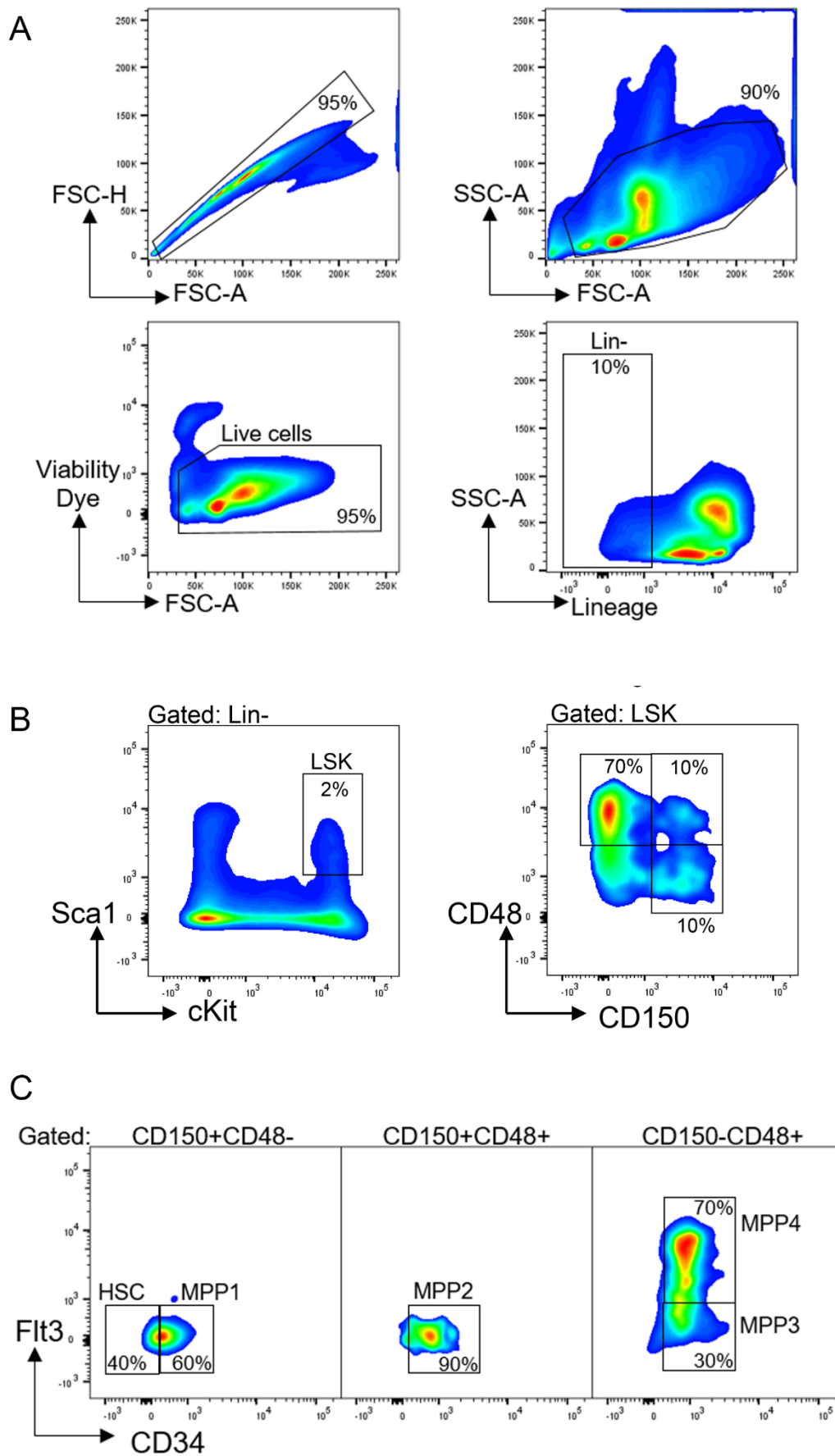


Figure S2

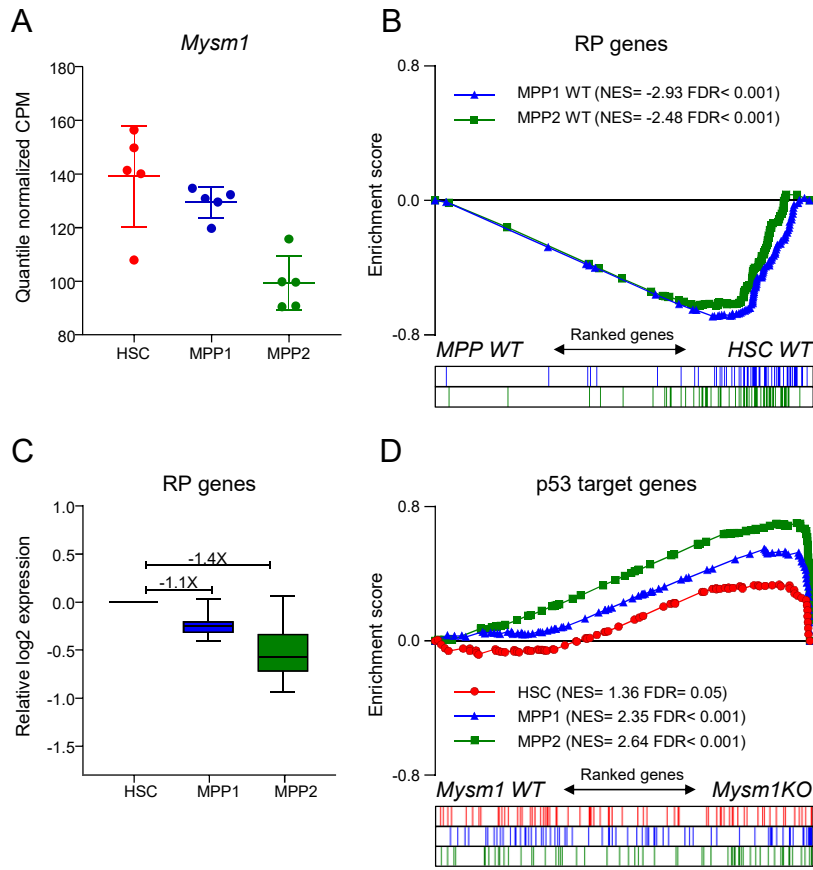
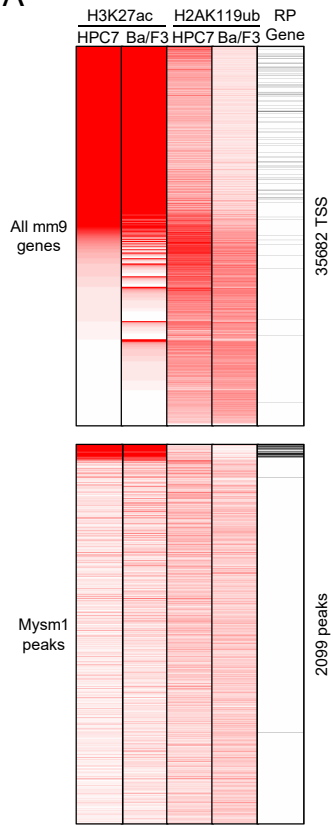


Figure S3

A



B

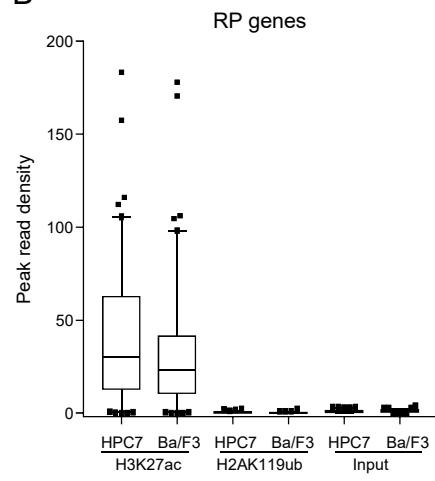
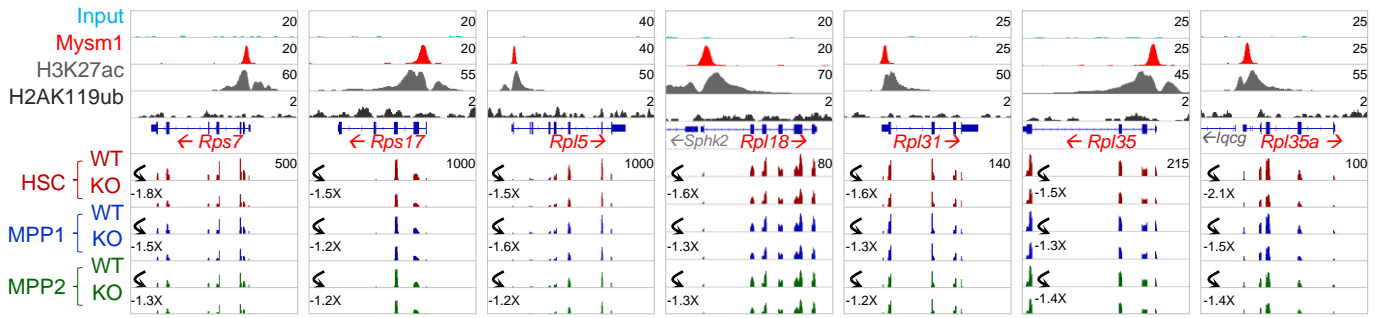
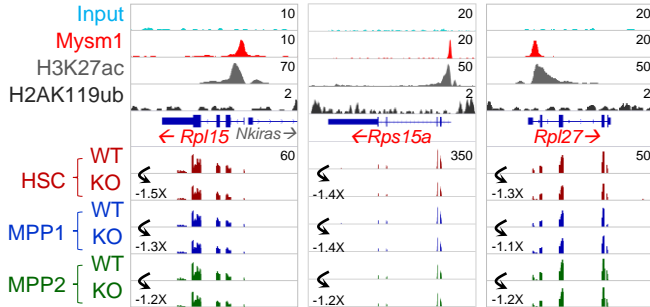


Figure S4

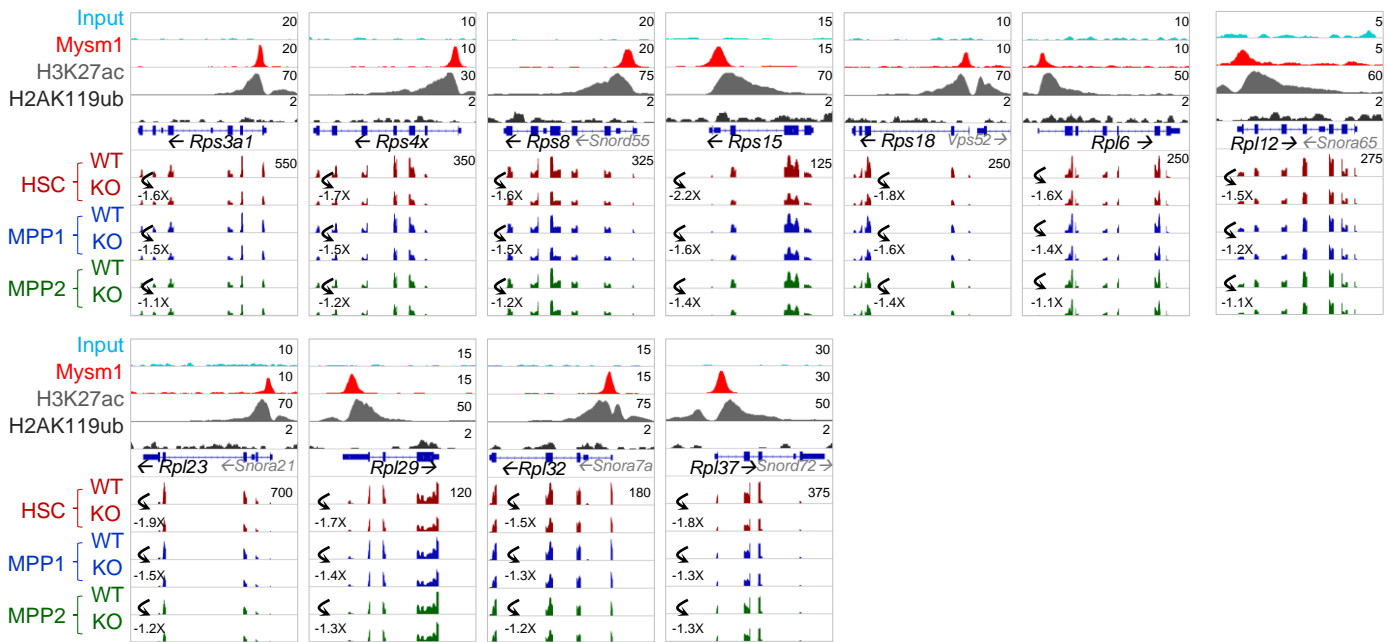
A. Additional Mym1-regulated DBA-causing *RP* genes



B. Mym1-bound DBA-causing *RP* genes (not significantly dysregulated)



C. Mym1-regulated non DBA-causing *RP* genes



D. Non Mym1-bound DBA-causing genes

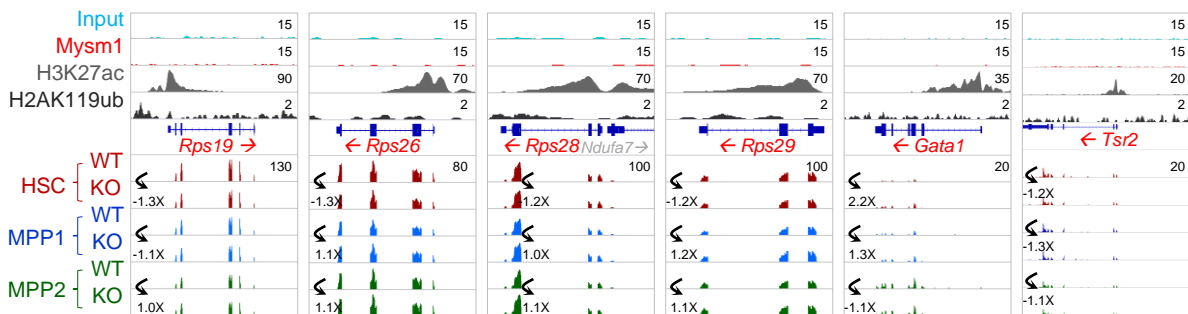


Figure S5

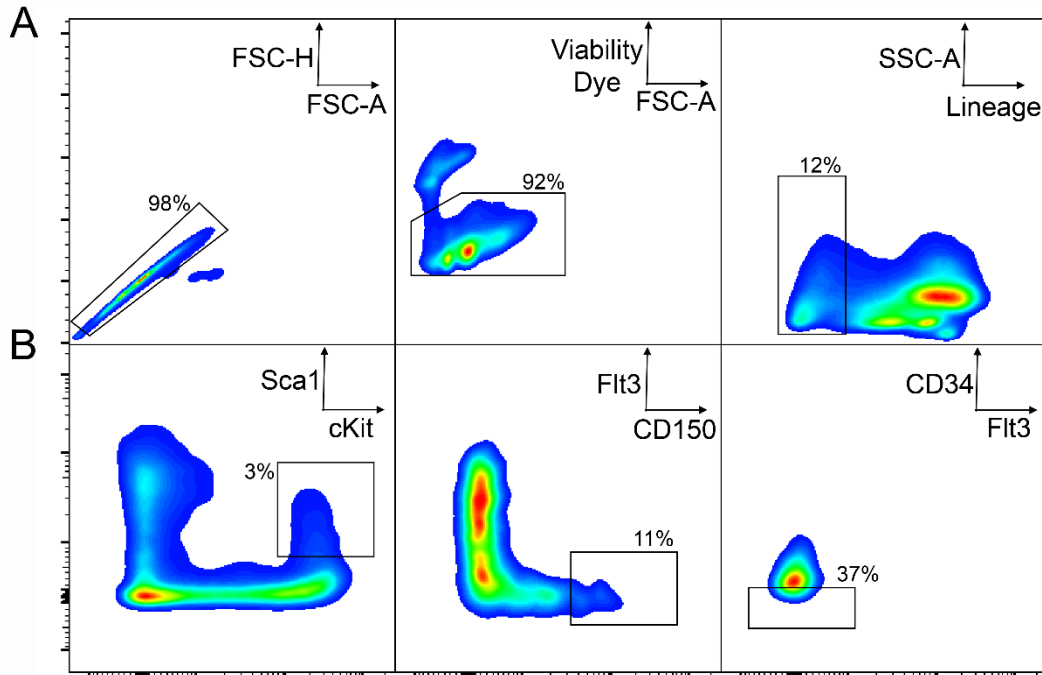


Figure S6

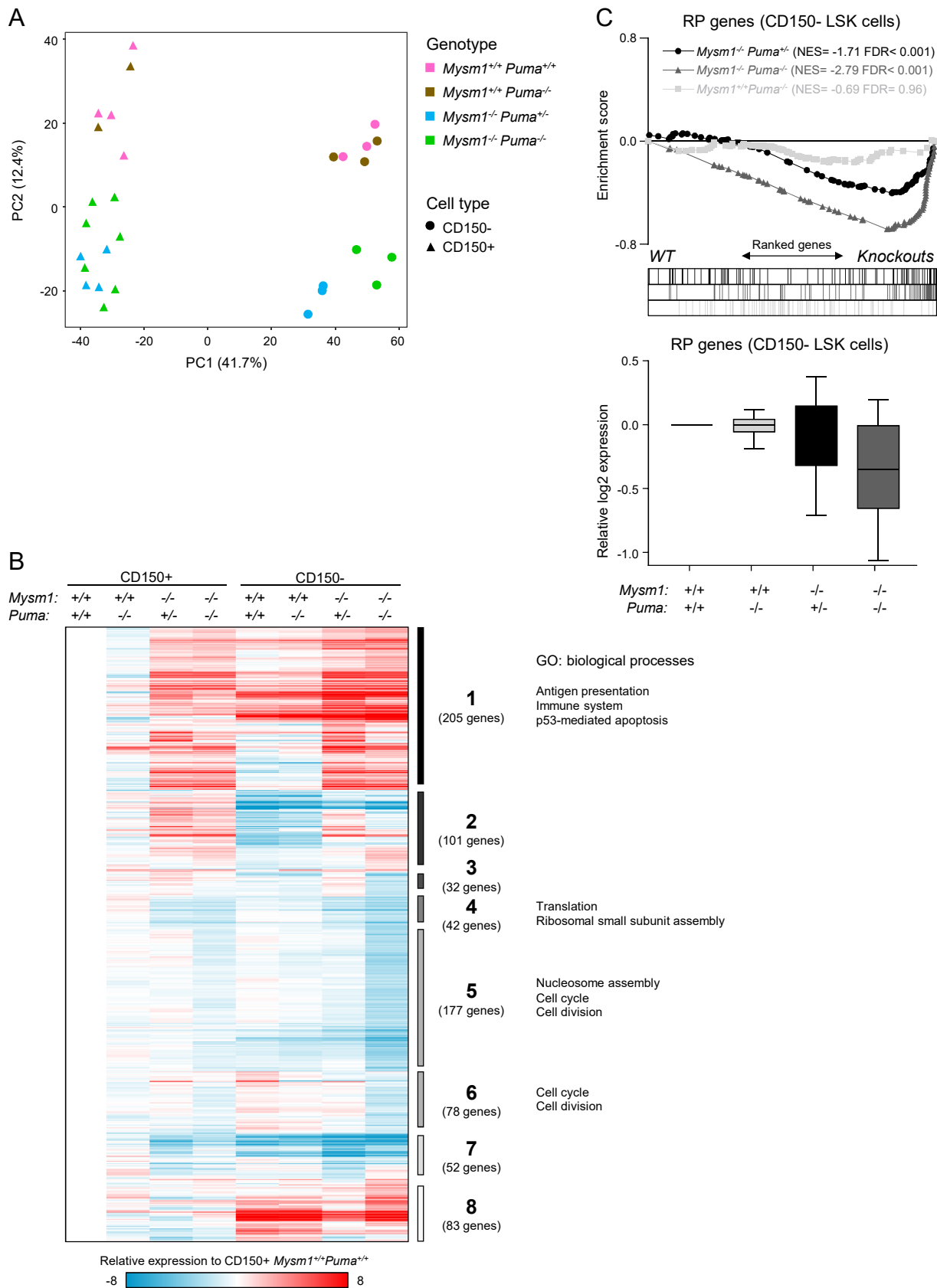


Figure S7

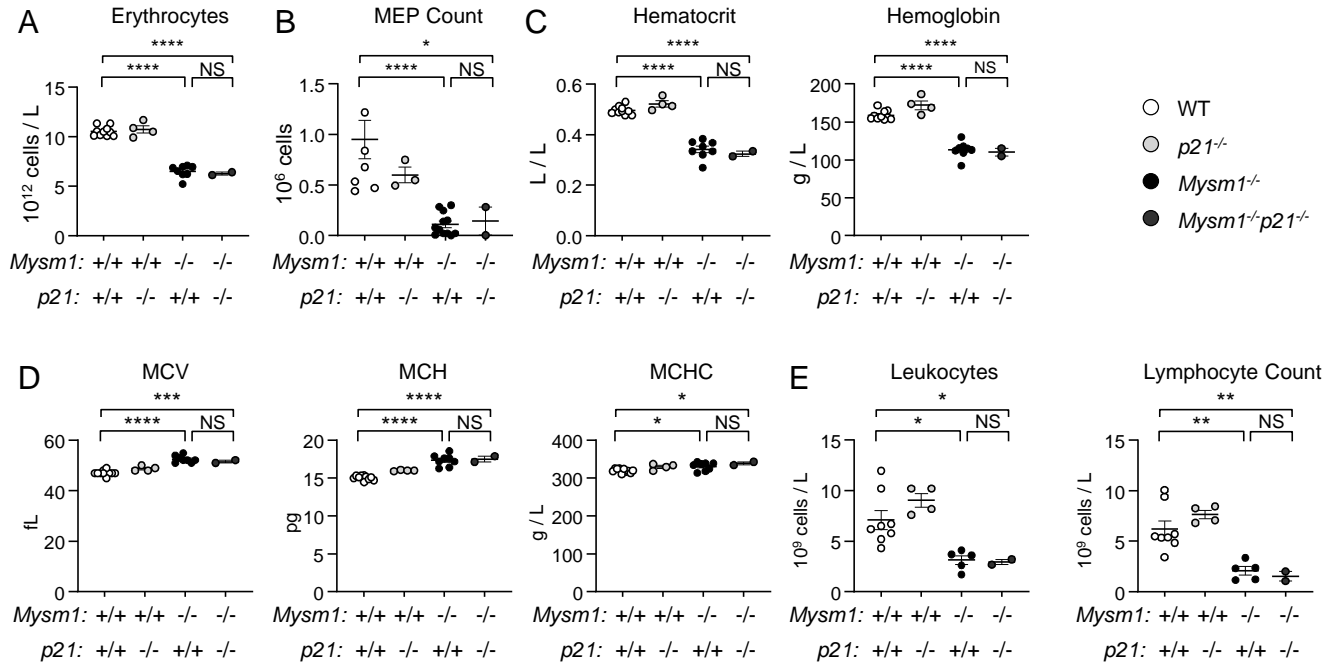


Figure S8

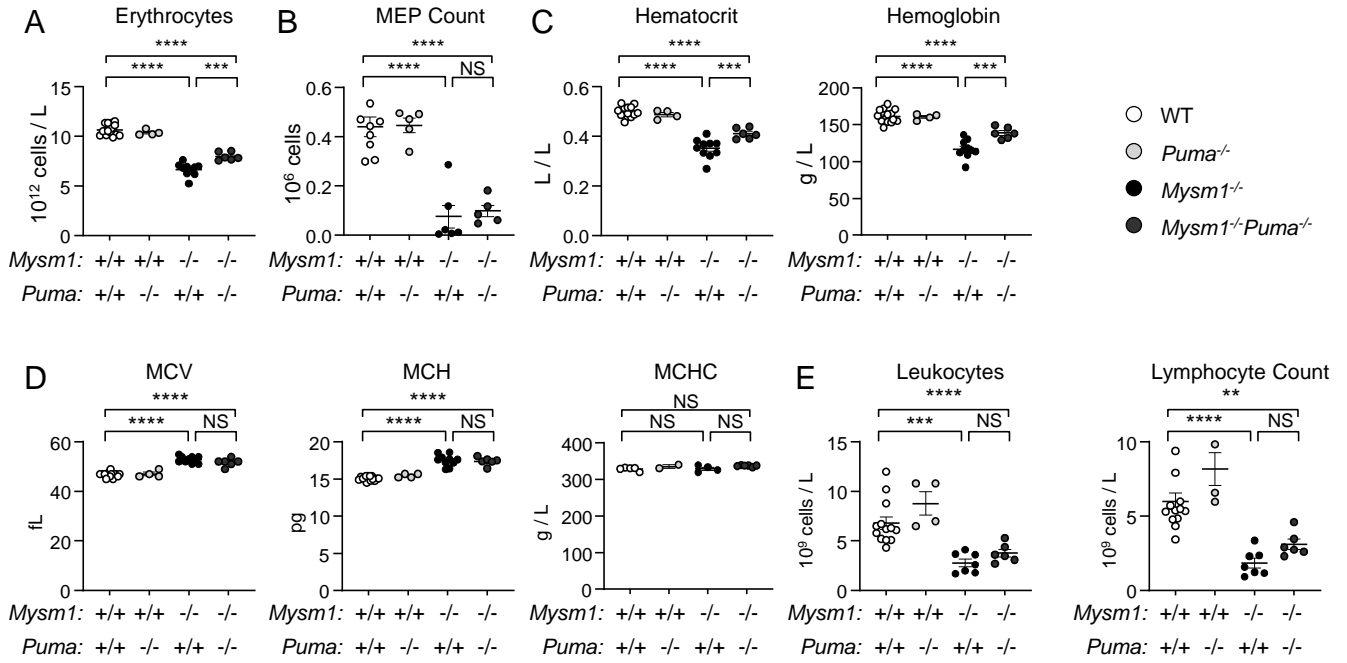


Figure S9

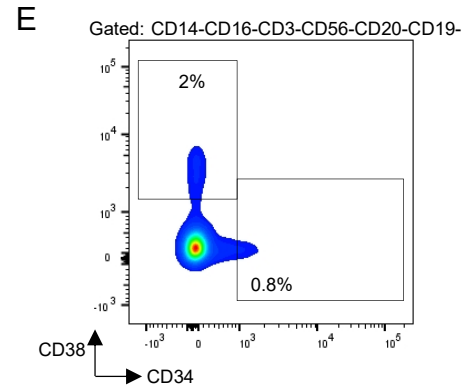
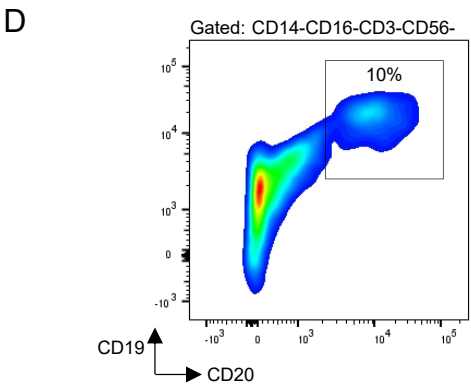
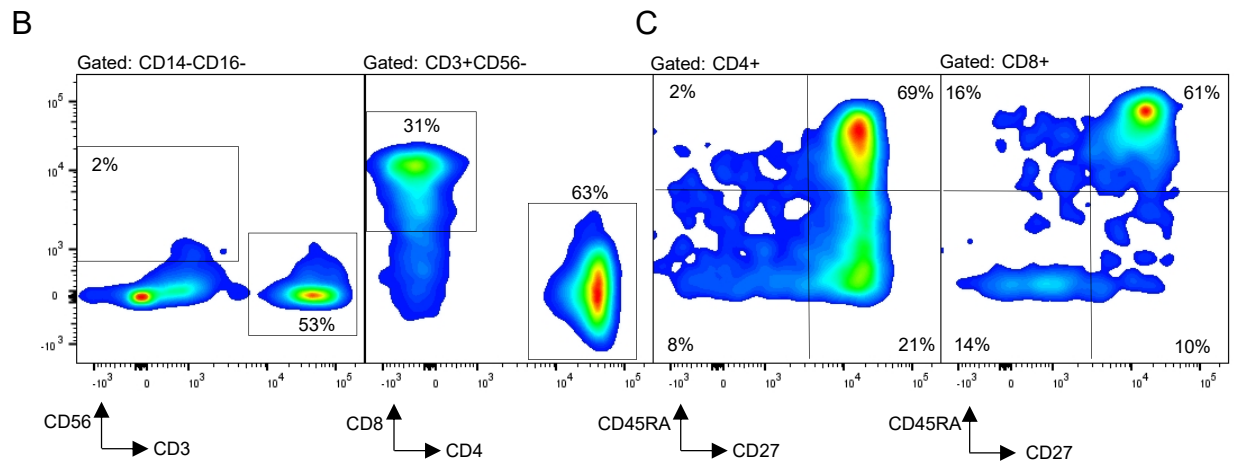
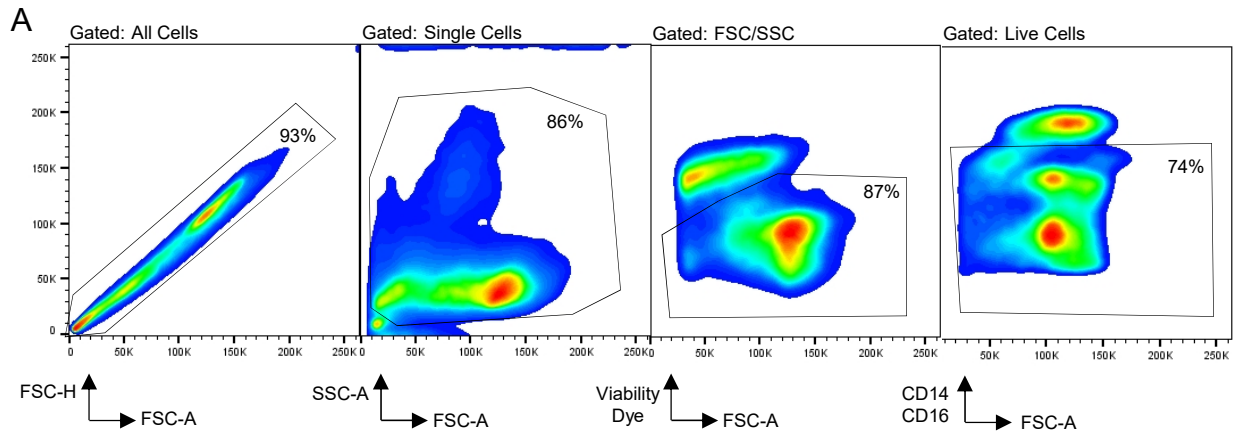


Figure S10

